Stretching Single-Stranded DNA: Interplay of Electrostatic, Base-Pairing, and Base-Pair Stacking Interactions

Yang Zhang,*† Haijun Zhou,‡ and Zhong-Can Ou-Yang*
*Institute of Theoretical Physics, The Chinese Academy of Sciences, Beijing 100080, China; †Laboratory of Computational Genomics, Donald Danforth Plant Science Center, St. Louis, Missouri 63141 USA; and ‡Theory Division, Max-Planck-Institute of Colloids and Interfaces, 14424 Potsdam, Germany

ABSTRACT Recent single-macromolecule observations revealed that the force/extension characteristics of single-stranded DNA (ssDNA) are closely related to solution ionic concentration and DNA sequence composition. To understand this, we studied the elastic property of ssDNA through the Monte Carlo implementation of a modified freely jointed chain (FJC), with electrostatic, base-pairing, and base-pair stacking interactions all incorporated. The simulated force-extension profiles for both random and designed sequences have attained quantitative agreements with the experimental data. In low-salt solution, electrostatic interaction dominates, and at low forces, the molecule can be more easily aligned than an unmodified FJC. In high-salt solution, secondary hairpin structure appears in ssDNA by the formation of base pairs between complementary bases, and external stretching causes a hairpin-coil structural transition, which is continuous for ssDNA made of random sequences. In designed sequences such as poly(dA-dT) and poly(dG-dC), the stacking potential between base pairs encourages the aggregation of base pairs into bulk hairpins and makes the hairpin-coil transition a discontinuous (first-order) process. The sensitivity of elongation to the base-pairing rule is also investigated. The comparison of modeling calculations and the experimental data suggests that the base pairing of single-stranded polynucleotide molecules tends to form a nested and independent planar hairpin structure rather than a random intersecting pattern.

INTRODUCTION

Throughout recent years, the new micromanipulation techniques combining high-force sensitivity (on the order of piconewtons (pN) and below) with accurate positioning (with precision on the order of angstroms) have offered researchers opportunities to directly manipulate individual biological macromolecules such as DNA and protein and to measure both intermolecular and intramolecular forces with high accuracy (see Smith et al., 1992, 1996; Cluzel et al., 1996; Strick et al., 1996; Rief et al., 1997; Lu et al., 1998; for recent reviews see Bustamante et al., 2000; Clausen-Schaumann et al., 2000). One of the main concerns of these experimental processes is the elastic response of a single biopolymer to an externally applied force field, i.e., the force/extension characteristic. Thanks to the intensive efforts from both experimentalists and theorists, it is now well established that the double-stranded DNA (dsDNA) exists with different force/extension regimes, stemming from its unique double-helix structures. For example, in the low-force regime, the elasticity of dsDNA is entropy dominated and the experimental force-extension data obtained with the magnetic bead method can be excellently described by the standard entropic worm-like chain model (Bustamante et al., 1994; Vologodskii, 1994; Marko and Siggia, 1995); in the high-force regime (starting as several tens of piconewtons), which is accessible with optical tweezers or atomic force microscopy, when the external force is comparable with the base-pair stacking interaction in dsDNA the polymers can be suddenly stretched to about two times its B-form length in a very narrow force range (Cluzel et al., 1996; Smith et al., 1996). An explanation of this regime is attributed to the short-ranged nature of base-pair stacking interaction. At large forces, the stacking potential can no longer stabilize the B-form configuration of dsDNA and the (optimally) stacked helical pattern is severely distorted (Zhou et al., 1999, 2000), and therefore a structural transition from canonical B-form to a new overstretched conformation called S-DNA is triggered.

With the mechanical features of dsDNA considerably understood, much attention was recently turned to single-stranded (ss)DNA or RNA molecules. As a linear chain of nucleotides with thin diameter and high flexibility, ssDNA (or RNA) is more contractile than dsDNA at low forces; however, it can be stretched to a greater length at high force because it no longer forms a helix. In 150 mM NaCl solution, the force/extension curve of a ssDNA melted from λ-phage DNA can be fit with a simple freely jointed chain (FJC) of Kuhn length 1.5 nm with an additional stretch modulus (Smith et al., 1996). Recent measurements showed that the elongation characteristics of ssDNA are very sensitive to the ionic concentration of solution, and the FJC model is not valid in both high ionic (e.g., 5 mM $MgCl_2$) and low ionic (e.g., 2 mM NaCl) solutions (Wuite et al., 2000; Bustamante et al., 2000; Maier et al., 2000). To explain the high-salt data, Montanari and Mezard (2000) proposed that secondary structure (hairpins) can be formed when ssDNA bends onto itself and its complementary bases are connected into base pairs, and it therefore needs a slightly

Received for publication 12 *February* 2001 *and in final form* 3 *May* 2001.
Address reprint requests to Dr. Yang Zhang, Donald Danforth Plant Science Center, Laboratory of Computational Genomics, 893 North Warson Road, St. Louis, MO 63141. Tel.: 314-812-8067; Fax: 314-812-8080; E-mail: yzhang@danforthcenter.org.

0006-3495/01/08/1133/11 $2.00

larger external force to pull open hairpinned ssDNA in the high-salt condition than that expected in FJC. Their calculation (Montanari and Mezard, 2000) showed that the hairpin-coil transition, when the pairing interaction is incorporated into FJC, is a continuous (second-order) process.

On the other hand, the measurement of Rief et al. (1999) shows that the force/extension characteristic of ssDNA is sequence dependent. When a (designed) poly(dA-dT) or poly(dG-dC) strand is pulled with an atomic force microscope, they found that at some stretched force (9 pN for poly(dA-dT) and 20 pN for poly(dG-dC)), the end-to-end distance of the designed molecules suddenly changes from nearly zero to a value comparable to its total contour length. This is drastically different from the gradual elongation of a ssDNA chain with a relatively random base composition (Maier et al., 2000). The present authors noticed that there is a higher probability for the paired bases to be neighboring in the designed ssDNA than that in the random sequence, and thus a strong vertical base-pair stacking interaction may exist in the designed ssDNA chain (Zhou et al., 2001). By including the effect of both base pairing and base-pair stacking interactions in the hairpinned FJC, it is has been showed that the force-induced hairpin-coil transition can be converted from a second-order into a first-order process (Zhou and Zhang, 2001).

Despite the partial success of FJC in describing the elastic property of ssDNA in the high-salt condition, no quantitative account of the experimental data of ssDNA in the low-salt condition (e.g., 2 mM NaCl) was performed in the above mentioned theoretic calculations. A major difficulty comes from how to appropriately take into account the (excluded volume) effects caused by the electrostatic interactions between charged phosphate groups along the ssDNA chain. Indeed, ssDNA is a highly negatively charged polyelectrolyte and the long-range electrostatically repulsive potential between segments may largely influence the conformations of stretched ssDNA, especially in the low-salt condition. Even in high ionic conditions as in the above experimental measurements in which electrostatic potential is considerably shielded, the residue repulsive potential may still influence the probability of formation of hairpin structure. So neglecting electrostatic interaction in high ionic conditions will also result in inaccurate estimations of important features of ssDNA, e.g., the magnitude and distance of pairing and stacking interactions of complementary bases.

In this work, our goal was a unified understanding of reported force/extension data of ssDNA molecules in different ionic atmospheres and for different nucleotide sequences through a Monte Carlo (MC) implementation of a modified FJC. Our treatment offers a computational rather than an analytical framework as previous approaches (Montanari and Mezard, 2000; Zhou and Zhang, 2001), thereby permitting a quantitative study of the effect of the long-range electrostatic interaction and various aspects of critical behaviors and the base-pairing rule of ssDNA systems. Our results show that, besides the inherent entropic elasticity in FJC, all of the other three interactions of electrostatics, base pairing, and base-pair stacking are necessary to be taken into account to gain a comprehensive understanding of the elastic behavior of ssDNA molecules in different environments.

In the next section, we at first determine the electrostatic interaction along the ssDNA through numerically solving the nonlinear Poisson-Boltzmann equation. We then describe the model of ssDNA and the MC procedure and present a direct comparison of our computed results and the experimental data concerned with the force/extension profile of ssDNA. The detailed discussions of the force-induced phase transition in the poly(dA-dT)/(dG-dC) system and the sensitivity of elongation characteristics to the base-pairing rule are also presented. We conclude with a brief summary of the main results of this work.

Electrostatic interaction between ssDNA segments

Under the assumptions that 1) the solute in a solution of strong electrolyte completely dissociates into ions and 2) all deviations of the solution from an ideal one (in which the ions distribute uniformly) are due to the electrostatic forces that exist between the ions, the electrostatic potential $\psi(\mathbf{r})$ of the solution at position $\mathbf{r}$ can be submitted to the Poisson-Boltzmann equation (Rice and Nagasawa, 1961):

$$\nabla^2\psi(\mathbf{r}) = -\frac{4\pi}{D}\sum_{i=1}^{n} v_i e c_i \exp(-v_i e\psi(\mathbf{r})/k_B T) \quad (1)$$

Here the solution is assumed to contain n different types of ions. The ith species has valence v_i, and the total number of ions of the ith type is N_i, with $c_i = N_i/V$ (V is the volume) being the bulk concentration of this species. D is the dielectric constant of the solution, and e denotes the protonic charge.

Equation 1 cannot be solved in closed form. Here we calculate the electrostatic potential of a ssDNA cylinder immersed in the solution of NaCl or $MgCl_2$ through numerically solving Eq. 1 according to the series expansion method that was first used by Pierce (1958). As an illustrative example, we show in Fig. 1 the electrostatic potentials of a ssDNA cylinder in 2 mM NaCl and 5 mM $MgCl_2$ solutions, where the potential function is expanded up to the 17th order for the symmetrical electrolyte (NaCl) and the 14th order for the asymmetrical electrolyte ($MgCl_2$) in our calculations (see Appendix).

However, such a numerical solution for a charged straight cylinder cannot be directly used on ssDNA, because this polymer actually takes a variety of irregular configurations in solution. One approach to the problem is to take the first-order approximation of Eq.1, i.e., Debye-Hükel form (see Eq. 12), the solution of which can be implicitly expressed. Around a point charge q, the electrostatic potential in Debye-Hükel approximation can be written as

$$\psi_{DH}(\mathbf{r}) = \frac{q}{D|\mathbf{r}|}\exp(-\kappa|\mathbf{r}|), \quad (2)$$

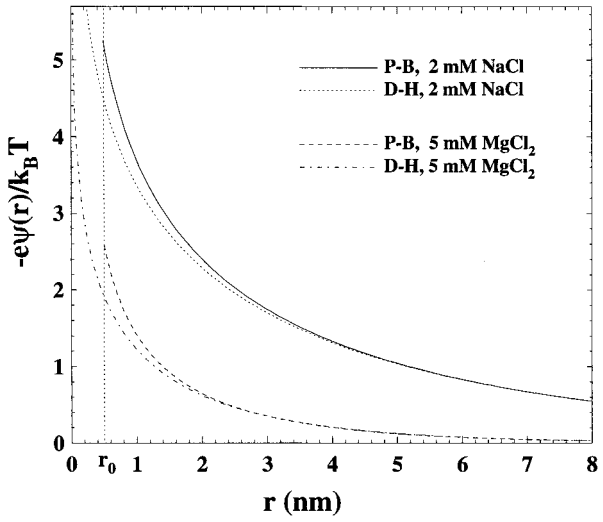

FIGURE 1 Electrostatic potential of ssDNA cylinder versus the radial distance from the cylinder axis in the solutions of 2 mM NaCl and 5 mM $MgCl_2$. The solid and dashed curves are, respectively, the numerical solutions of Poisson-Boltzmann equation (P-B) up to the expansion order $m = 17$ for NaCl and $m = 14$ for $MgCl_2$ in Eq. 13; the dotted and dash-dotted curves denote corresponding Debye-Hükel approximations (D-H) with effective linear charge density ν along the axis listed in Table 1. The vertical dotted-line at $r_0 = 0.5$ nm corresponds to the surface of the ssDNA cylinder.

where $\mathbf{r}$ is the position vector from this charge, and the inverse Debye length κ is equal to $(8\pi c_0 e^2/Dk_BT)^{1/2}$ (for NaCl solution) or $(24\pi c_0 e^2/D_BT)^{1/2}$ (for $MgCl_2$).

To count the influence of higher expansion terms of the Poisson-Boltzmann equation, one can phenomenologically change the amplitude of the Debye-Hükel potential of Eq. 2 to match the precise solution of the Poisson-Boltzmann equation (Brenner and Parsegian, 1974; Stigter, 1977). According to Eq. 2, at radial distance r the electrostatic potential of a uniformly charged straight cylinder of infinite length is

$$\psi_{DH}(r) = \int_{-\infty}^{\infty} \frac{\nu d\lambda}{D} \frac{\exp(-\kappa\sqrt{\lambda^2 + r^2})}{\sqrt{\lambda^2 + r^2}} = \frac{2\nu}{D} K_0(\kappa r), \quad (3)$$

where λ is arc length along the cylinder axis, ν is effective linear charge density, and K_0 is the first-order modified Bessel function (Gradshteyn and Ryzhik, 1980). By comparing Eq. 3 with the Poisson-Boltzmann solution in the overlap region far from the cylinder surface as shown in Fig. 1, we can determine the effective linear charge density ν in different bulk ionic concentration c for both the NaCl and the $MgCl_2$ solution (see Table 1). In Table 1 we also show the effective charge density of dsDNA.

As shown in Fig. 2, all the data of ν can be very well fitted by the formula of

$$\nu = \exp(\alpha + \beta c^{2/5}), \quad (4)$$

TABLE 1 The effective linear charge density ν (in unit of e/nm) of DNA molecules, calculated from the comparison of the Poisson-Boltzmann solution and the modified Bessel function

Ionic concentration	ssDNA		dsDNA	
c_0 (M)	NaCl	$MgCl_2$	NaCl	$MgCl_2$
1.	4.18	9.50	91.85	993.16
0.75	3.50	6.74	56.15	410.67
0.5	2.84	4.51	31.22	144.10
0.2	2.04	2.31	11.73	24.52
0.15	1.89	1.97	9.29	16.22
0.1	1.73	1.64	7.02	9.82
0.05	1.53	1.27	4.78	4.98
0.02	1.37	0.99	3.29	2.66
0.01	1.29	0.86	2.66	1.91
0.005	1.23	0.78	2.26	1.45
0.002	1.17	0.71	1.93	1.13
0.001	1.14	0.67	1.76	1.00
α	0.0338	−0.577	0.300	−0.505
β	1.36	2.80	4.18	7.33

α and β are the parameters of Eq. 4 fitted to the data of ν (see Fig. 2).

with the fitting parameters α and β listed also in Table 1.

It should be mentioned that the full linear charge density has been assumed in our calculation; i.e., the effect of counterion charge is not taken into account here. For dsDNA, this effect can lead a reduction of the real charge of the polymer in NaCl solution by a factor of ~0.73 according to Stigter's electrophoresis theory (Schellman and Stigter, 1977; Stigter, 1977). As a comparison, we also show in Fig. 2 Stigter's calculation for dsDNA in NaCl solution, where 73% of electrophoretic charge was assumed (Stigter, 1977; Stigter and Dill, 1993). These results show that the value of ν here is not very sensitive to the uncertainties of the electrophoretic charge.

MODEL AND METHOD OF CALCULATIONS

Model of single-stranded DNA

In the simulation, the ssDNA molecule is modeled as a FJC with N elastic bonds. The conformation of the chain is specified by the space positions of its vertices, $\mathbf{r}_i = (x_i, y_i, z_i)$, $i = 0,1,\ldots,N$, in a three-dimensional Cartesian coordinate system with $\mathbf{r}_0$ fixed at the original point. The equilibrium features of a ssDNA in solution is determined by the interplay of the following five energies.

The first energy, E_{ele}, is the electrostatic interaction energy among the negatively charged phosphate groups along the ssDNA chain. As discussed in the last section, the electrostatic energy of ssDNA can be calculated according to the Debye-Hükel approximation:

$$\frac{E_{ele}}{k_BT} = \frac{\nu^2}{k_BTD} \int d\lambda_i \int d\lambda_j \frac{\exp(-\kappa|\mathbf{r}_i - \mathbf{r}_j|)}{|\mathbf{r}_i - \mathbf{r}_j|}, \quad (5)$$

where the effective charge density ν is taken from Table 1 and the integrations are done along the chain; $|\mathbf{r}_i - \mathbf{r}_j|$ is the distance between two charges at arc length parameters λ_i and λ_j along the chain.

The second energy, E_{pair}, results from the pairing potential between complementary bases. Two elementary pairings are the G-C and A-T base pairs of

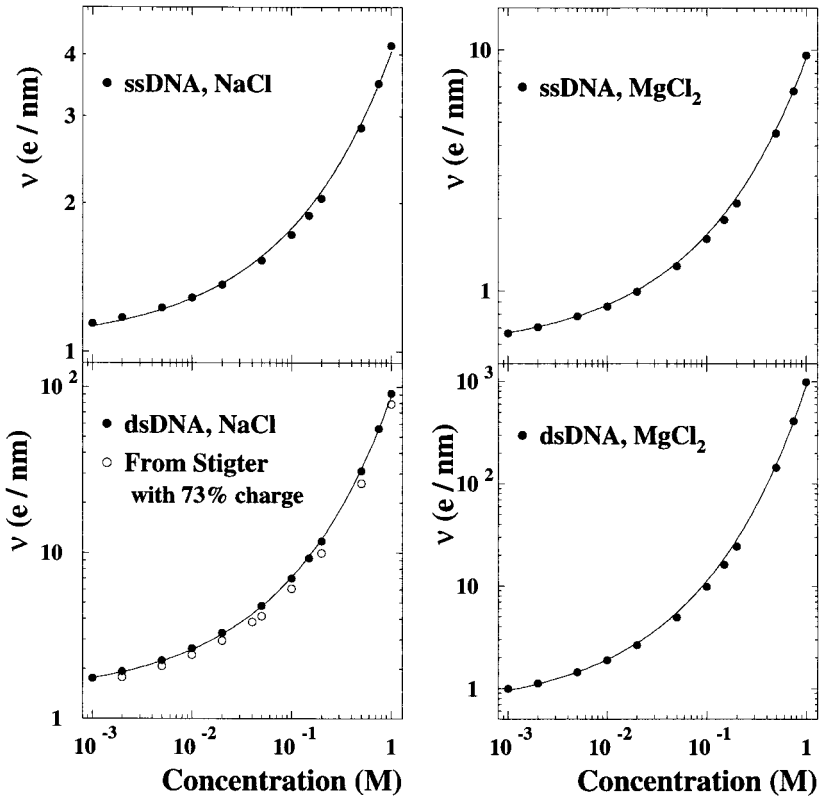

FIGURE 2 The effective linear charge density ν for ssDNA and for dsDNA at different ionic concentrations of NaCl or $MgCl_2$: ●, results of the present work; ○, Stigter's results (Stigter, 1977; Stigter and Dill, 1993), where electrophoretic charge of $-0.73e$ were used (which was required to fit the electrophoresis theory to experimental data). In the present calculation, the full charge per phosphate group is assumed. The curves are drawn according to Eq. 4 with parameters listed in Table 1.

Watson and Crick. As a G-C pair is formed through the formation of three hydrogen bonds whereas an A-T one involves only two hydrogen bonds, the base-pairing potential is sequence dependent. Because the Kuhn length of ssDNA (~1.5 nm) is longer than the length of the sugar-phosphate backbone between two adjacent bases, each node (vertex) in our model actually includes several bases. We approximate the base-pairing interaction by the node-pairing energy of $E_{pair} = \Sigma_{i=1}^{N_P} V_p$, where N_P is the number of node pairs and V_P is a sequence-dependent parameter denoting the intensity of a certain pairing mode. The pairing rule in our following simulation is similar to the standard one that keeps only nested structure (Bundschuh and Hwa, 1999; Higgs, 1996; Montanari and Mezard, 2000; Zhou and Zhang, 2001): 1) two nodes (i, j) can be paired only when their distance $|\mathbf{r}_i - \mathbf{r}_j|$ is less than 2 nm, which corresponds approximately to the interaction range of Watson-Crick hydrogen bond in dsDNA (Saenger, 1984); 2) each node can be paired to at most one other node; 3) two node pairs (i, j) and (k, l) can coexist only when they are either nested (i.e., $i < k < l < j$) or independent (i.e., $i < j < k < l$); and 4) $|j - i| \geq 4$; this restriction permits flexibility of the chain and it is also necessary to rule out entirely the influence of phase space on the number of pairings, as confirmed by our following MC simulations. Condition 3 rules out the possibility of formation of pseudo-knots that belong to the tertiary structure of polynucleotides. As we will show, it also takes an important role in the determination of the force/extension feature of ssDNA.

The third energy, E_{sta}, comes from the vertical stacking interactions between neighboring base pairs. We calculate the stacking energy by $E_{sta} = \Sigma_{i=1}^{N_S} V_s$, where N_S is the number of stacked node pairs and V_S is the interactive potential between two neighboring node pairs. Two node pairs are considered as stacked only when they are nearest neighbors to each other, namely, (i, j) and $(i + 1, j - 1)$.

The fourth energy in our model is that needed to make the bond length between two consecutive vertices to deviate from the equilibrium value. It can be written as

$$E_{ela} = \frac{1}{2} \sum_{i=1}^{N} Y(|\mathbf{r}_i - \mathbf{r}_{i-1}| - b)^2, \quad (6)$$

where b is the Kuhn length for ssDNA and Y characterizes the stretch stiffness of the ssDNA backbone

The fifth energy, i.e., work done by the external force F, is written as $E_{for} = -Fz_N$, where z_N is the z-coordinate of the last vertex. (In the simulation we choose the orientation of the external force F to be along the z axis.)

Monte Carlo procedure

To investigate the equilibrium thermodynamics of stretched ssDNA molecules, we produce by computer a canonical ensemble of DNA conformations for each given force, through the realization of a Markov process by the Metropolis procedure (Metropolis et al., 1953). The conformation of the ssDNA chain is initially generated by a random walk with step length of b and afterwards is driven by the following four types of movements.

Movement I involves a rotation of an interval subchain containing an arbitrary amount of linkers around the straight line connecting the vertices bounding the subchain by an angle η_1. In movement II, a subchain between a chosen vertex and the free end is rotated around an axis with arbitrary orientation by an angle η_2. In movement III, the bond length l_i of a randomly chosen linker is changed into a new value of $l_i(1 + \eta_3)$. The value of η_i $(i = 1, 2, 3)$ is uniformly distributed over the interval $(-\eta_i^0, \eta_i^0)$, where η_i^0 is chosen to guarantee that about half of the trial moves of the ith type are accepted (Zhang et al., 2000).

The fourth type of movement (movement IV) involves a permutation of a randomly chosen two-segment subchain (e.g., the subchain from nodes i to $i + 2$) and another randomly chosen three-segment subchain (e.g., the subchain from node j to $j + 3$), which was first adopted by Vologodskii et al. (1992) in

the MC calculation of supercoiled dsDNA. Because the length of doublet subchain ($|\mathbf{r}_i - \mathbf{r}_{i+2}|$) and the length of triplet subchain ($|\mathbf{r}_j - \mathbf{r}_{j+3}|$) are usually unequal, to perform the permutation, we should at first deform the conformations of both doublet and triplet subchains so that the length of these subchains could be incorporated to their new positions. More specifically, the doublet subchain should be deformed and shifted to the position [$\mathbf{r}_j$, $\mathbf{r}_{j+3}$] and the triple subchain to the position [$\mathbf{r}_i$, $\mathbf{r}_{i+2}$]. The net result of this permutation is a translation of the randomly chosen subchain (between node *i* and node *j*) by one segment along the chain axis. Even though the acceptance probability of this movement can be quite low, it can substantially increase the probability of extrusion and resorption of hairpinned structures and help the simulation to go out of some local traps.

All of the above four types of movements satisfy the basic requirement of the Metropolis procedure of microscopic reversibility; i.e., the probability of trial conformation *B* when current conformation is *A* must be equal to the probability of trial conformation *A* when current conformation is *B*. A trial move from a conformation *A* to another conformation *B* is accepted on the basis of the probability $p_{A\to B} = \min[1, \rho(E_B)/(\rho(E_A)]$, where $E_{A(B)}$ and $\rho(E_{A(B)})$ are, respectively, the total energy and probability weight factor of conformation *A*(*B*). In the canonical Metropolis algorithm, the energetic importance sampling is realized by choosing the probability weight factor $\rho(E)$ as the Boltzmann weight factor: $\rho(E) = \exp(-E/k_BT)$, where the total energy is $E = E_{ele} + E_{pair} + E_{sta} + E_{ela} + E_{for}$ in our model. However, the energy landscape of ssDNA with hairpin structures is characterized by numerous local minima separated by energy barriers, and the probability of the canonical Metropolis procedure to cross the energy barrier of height ΔE is proportional to $\exp(-\Delta E/k_BT)$. When the pairing and stacking energies are rather large, e.g., in the case of poly(dG-dC), the energy barriers around some special conformations can be very high so that the simulation tends to get trapped in these conformations, although they are by no means of the lowest energy. During the finite CPU time, only small parts of the canonical ensemble of DNA conformations can therefore be explored, rendering the calculation of physical quantities unreliable.

To overcome this problem of ergodicity breaking of poly(dG-dC) ssDNA, we produce an artificial ensemble according to a modified weight factor (Zhang, 2000):

$$\rho(E) = \exp\left[\left(-E + \frac{\sqrt{2}}{\sigma}|E - \langle E\rangle|\right)\Big/ k_BT\right], \qquad (7)$$

where $\sigma^2 = n_F/2$ is the mean squared derivation of energy of the canonical thermodynamic system, and n_F the number of degrees of freedom of the chain, $\langle E\rangle$ is the averaged energy of the system that can be calculated in a simple iteration procedure (Hansmann and Okamoto, 1997; Zhang, 2000). In Eq. 7, the probabilities of both high and low energy are exponentially reinforced, and the sharp peak of the canonical ensemble around $\langle E\rangle$ is damped, which can efficiently help the simulation to jump out from local energy basins.

Because one configuration in the artificial ensemble of Eq. 7, in fact, represents $n(E) = \exp[-\sqrt{2}|E - \langle E\rangle|/(k_BT\sigma)]$ configurations in canonical system, we should reweight the artificial sample to obtain the expectation value of considered quantity. For example, the averaged extension z_N should be calculated by

$$\langle z_N\rangle = \frac{\sum_{i=1}^{N_{MC}} z_N(E_i)n(E_i)}{\sum_{i=1}^{N_{MC}} n(E_i)}, \qquad (8)$$

where N_{MC} is the number of sweeps of the artificial sample.

RESULTS AND DISCUSSION

Force/extension of ssDNA

There are three groups who have pulled ssDNA of both random and designed sequences and presented their force/extension data in different salt environments (Smith et al., 1996; Rief et al., 1999; Wuite et al., 2000; Maier et al., 2000; Bustamante et al., 2000). These data offer us good opportunity to check the theoretical model and meanwhile determine the four main parameters in our model, i.e., Kuhn length *b*, stretching modulus *Y*, pairing potential V_P, and stacking potential V_S (see Table 2). In the following presented calculations, we make 20,000,000 MC runs with $N = 100$ nodes at each given external force for each case. We have also confirmed that using a larger value of *N*, e.g., $N = 200$, with more MC runs does not lead to different results.

TABLE 2 Parameters used in our modeling calculation to fit the data presented in Fig. 3

Sequence	V_P (k_BT)	V_S (K_BT)	*b* (nm)	*Y* (k_BT/nm^2)
Random	4.6	0	1.6	123.5
Poly(dA-dT)	4.1	4.0	1.6	123.5
Poly(dG-dC)	10.4	6.0	1.6	123.5

We first calculate the force/extension characteristics of FJC with elastic bonds but without pairing and stacking interactions. As shown in Fig. 3 *a*, the electrostatic interaction tends to swell the volume occupied by the chain and make the segments more easily aligned along the force direction. This is equivalent to enlarging the Kuhn length of ssDNA. The lower the ionic concentration becomes, the larger the effective Kuhn length is and the more rigid the molecule looks. However, at large forces where the polymer comes to be straight enough, the force/extension curves for a FJC with and without electrostatic interaction coincide with each other, indicating that in this region the electrostatic interaction is no longer important and the extension is mainly caused by elongation of the elastic bonds. By a direct comparison with experimental data, we can determine the stretching modulus of the sugar-phosphate backbone of ssDNA to be $Y = 123.5k_BT/nm^2$.

Now consider the effects of pairing interaction in ssDNA. In Fig. 3 *b* is the force/extension data of a plasmid ssDNA fragment of 10.4 kb in 5 mM $MgCl_2$ or 2 mM NaCl solution. Bearing in mind that the sequence is relatively random and the formed base pairs in ssDNA are usually separated spatially from each other along the molecule, the stacking interaction is negligible in this case. We therefore take the stacking potential $V_S = 0$. The best fit to the data is $V_P = 4.6k_BT$ and $b = 1.6$ nm. In lower salt concentration, 2 mM NaCl, the force-elongation curve is not influenced much by the pairing potential with the comparison of Fig. 3 *a*, because the dominant electrostatic repulsive potential excludes the bases from getting close to pairing interaction range and the node-pairing probability is very rare. However, in a high-salt solution of 5 mM $MgCl_2$, the force/extension property is the result of completion of two opposite interactions of pairing and electrostatic repulsive interactions. The experimental data suggest that the pairing effect is slightly larger at low force in this case.

In the cases of designed poly(dA-dT) or poly(dG-dC) ssDNA, the unitary base pairs of A-T or G-C can be formed in

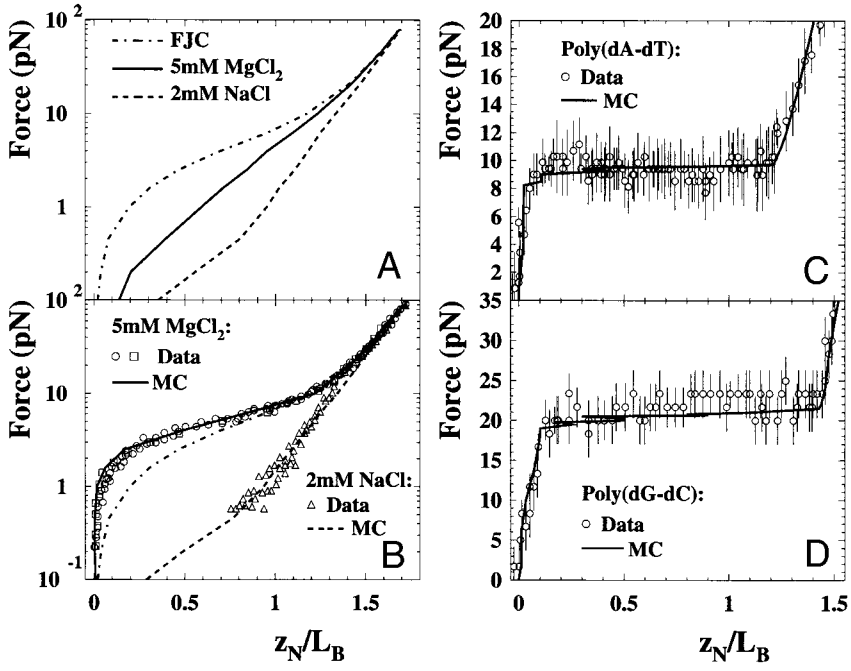

FIGURE 3 External force as the function of distance of two ends of ssDNA, scaled by its B-form length L_B. $L_B = Nb/1.58769$ in the modeling calculation, and other model parameters used in our Monte Carlo calculation are listed in Table 2. (*a*) Monte Carlo results of pure freely jointed chain (FJC) without electrostatic, pairing and stacking potential (dash-dotted line) and that with electrostatic interaction considered in 2 mM NaCl (- - -) and 5 mM $MgCl_2$ (——) solutions, but $V_P = V_S = 0$. (*b*) λ-Phage DNA in 2 mM NaCl and 5 mM $MgCl_2$ solutions. Data are taken from Bustamante et al. (2000) (△ and □) and from Maier et al. (2000) (○). (*c* and *d*) For designed poly(dA-dT) and poly(dG-dC) sequences, respectively, in 150 mM NaCl solution. Data are taken from Rief et al. (1999), where the extension of ssDNA is obtained by $z_N/L_B = 1.58769(L - L_1)/(L_2 - L_1)$. Here L is the total extension of both dsDNA and ssDNA (see Fig. 3 in Rief et al. (1999)). For poly(dA-dT), $L_1 = 60$ nm and $L_2 = 545$ nm; for poly (dG-dC), $L_1 = 257$ nm and $L_2 = 525$ nm.

respective sequences. Because it is possible for the formation of long stems of stacked base pairs, stacking potential should be included in discussing its configurational properties. As shown in Fig. 4, the stacking potential can dramatically change the conformation of ssDNA at low force. When the stacking potential is absent, the base pairs are formed quite randomly with formation of many interior loops and branched structures. So the dispersed hairpin structure can be easily pulled open in

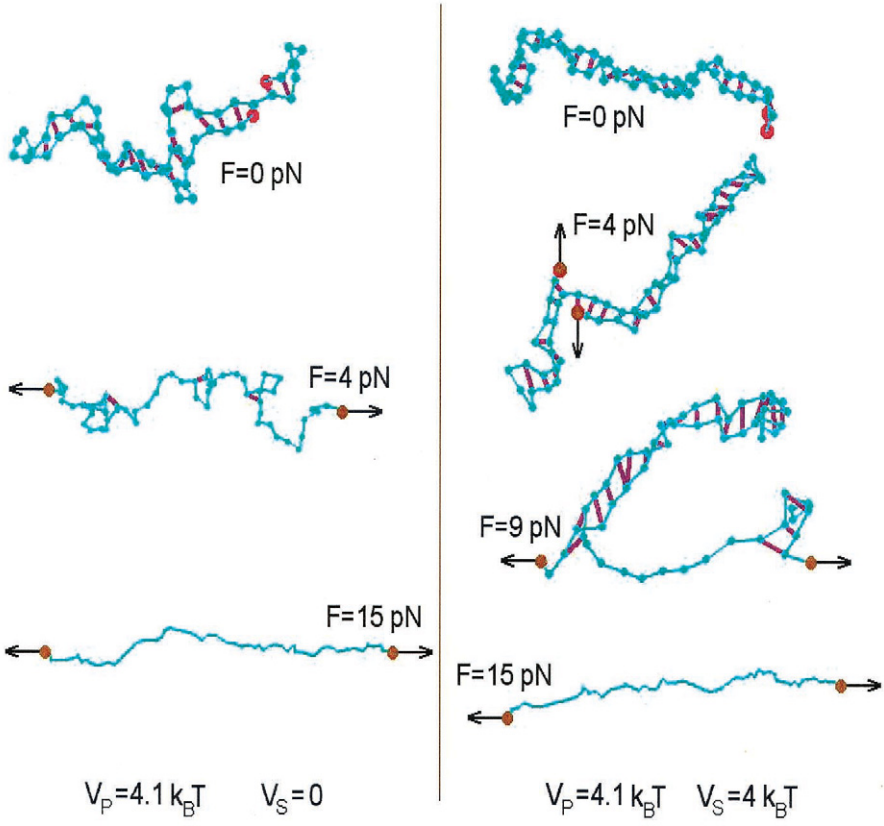

FIGURE 4 The typical conformations of ssDNA chains with random sequence (*left*) and designed poly(dA-dT) sequence (*right*) in 150 mM NaCl solution stretched at different external forces, which are produced in the Monte Carlo simulations of $N = 60$. The fictitious bases and backbone are expressed by green nodes and lines, with the nodes of two ends denoted by two bigger red globes. The hydrogen bonds of base pairs are denoted by magenta short lines.

a medium force (see the left column of Fig. 4). When the stacking interaction exists, on the other hand, the base pairs are encouraged energetically to be neighboring and therefore lead to the formation of bulk hairpin structure (see the right column of Fig. 4). A threshold force is needed to pull back the bulk hairpin structure (see Fig. 3, *c* and *d*), and the transition from hairpin to coil is abrupt. The value of threshold force, i.e., the height of the plateau in the force/extension curve, is dependent on the pairing and stacking potentials of the nodes. The best fit to the data, as in Fig. 3, *c* and *d*, are $V_P = 4.1k_BT$ and $V_S = 4k_BT$ in poly(dA-dT) sequence, $V_P = 10.4k_BT$ and $V_S = 6k_BT$ in poly(dG-dC) sequence.

Transition criticality in designed ssDNA

It has been shown from force/extension data that the elongation of natural ssDNA with a random sequence under external force is gradual, but that of designed sequence is in a cooperative and discontinuous manner when a stacking interaction is involved. This first-order-like phase transition of the designed ssDNA system can also manifest itself in other aspects.

In Fig. 5 *a* we present the average number of pairings scaled by the maximum pairing number of $(N - 2)/2$ for poly(dA-dT) sequence in 150 mM NaCl. When the external force is smaller than the critical force ($F_c \approx 9.5$ pN), the number of pairing $2N_P/(N - 2) \approx 1$, suggesting that almost all the bases are paired. The number of stacked pairs N_S also reaches its maximum value and signifies that all the pairs aggregate into a compact pattern. Around the external force F_c, the bulk hairpin is pulled back abruptly (in the sense that during this process the force keeps constant), and the numbers of pairings and stackings sharply decrease from their maximum to zero. This behavior is a reminiscence of temperature-induced discontinuous transition in, e.g., a two-dimensional spin system as described by the Ising model. But there the order parameter is magnetization or number of spins with specified orientation (see, e.g., Wilde and Singh, 1998). And here the order parameter is number of paired bases, and the transition is force induced and takes place in a one-dimensional system.

The electrostatic energy of ssDNA also changes with external force in a cooperative manner (Fig. 5 *b*) because of the discontinuous jump of the averaged distance between charged nodes at the critical point. One can notice that there are irregular doglegs for the values of the average extension, the number of pairings, and the value of the electrostatic energy as the external force approaches the critical point. This is because of the so-called critical fluctuation in our simulations at the critical point. In Fig. 6 is shown the time series of some order quantities such as the extension z_N and number of pairings. These quantities stay around their values of thermodynamic equilibrium when the external force is away from the critical point. When the external force approaches F_c, however, the fluctuations of their value sharply enlarge, because the correlation length is expected to diverge at this point.

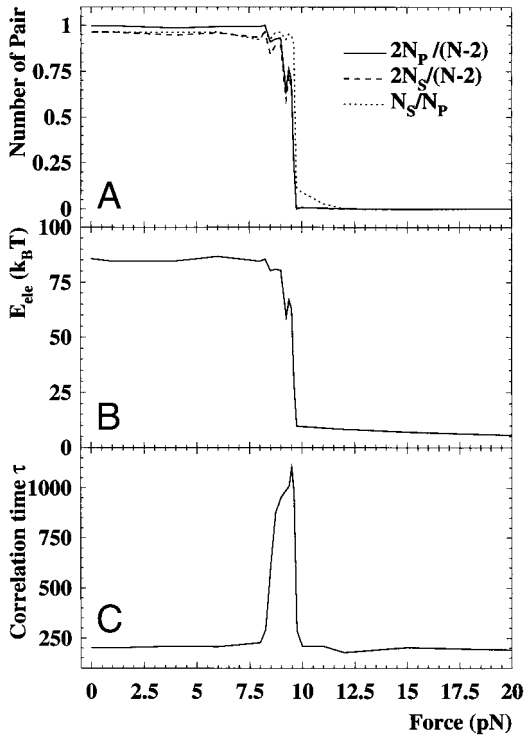

FIGURE 5 The order parameters and autocorrelation time as the function of external force for poly(dA-dT) sequence in 150 mM NaCl solution. (*a*) Number of node-pairs (N_P), stackings (N_S), and the ratio of pairings and stackings, all of which are scaled be the maximum value of pairings of $(N - 2)/2$. (*b*) Electrostatic Debye-Hükel potential. (*c*) The autocorrelation time of extension of ssDNA polymer calculated by Eqs. 9 and 10. The MC time is scaled by the number of nodes N.

To confirm this point, we calculate the integrated autocorrelation time τ of the extension z_N:

$$\tau = \int_0^\infty \frac{\chi(t)}{\chi(0)}\, dt, \tag{9}$$

where time t, i.e., MC steps, is scaled by the magnitude N of the chain, and the time-displaced autocorrelation function $\chi(t)$ is calculated as

$$\chi(t) = \int_0^{t_{max}-t} dt'[z_N(t') - \langle z_N\rangle][z_N(t' + t) - \langle z_N\rangle]. \tag{10}$$

In Eq. 10, t_{max} is the total time sweeps of MC simulation, and $\langle \ldots \rangle$ denotes the time average along the MC series.

Fig. 5 *c* shows how the correlation time τ changes with external force. At a critical point, the correlation time indeed diverges. So the number of independent measurements, $n = t_{max}/2\tau$, is very small in the simulation, which renders the MC calculation at the critical point unreliable. This effect, known as critical slowing down, is an inherent property of the MC algorithm used to perform the simulation for a phase transition

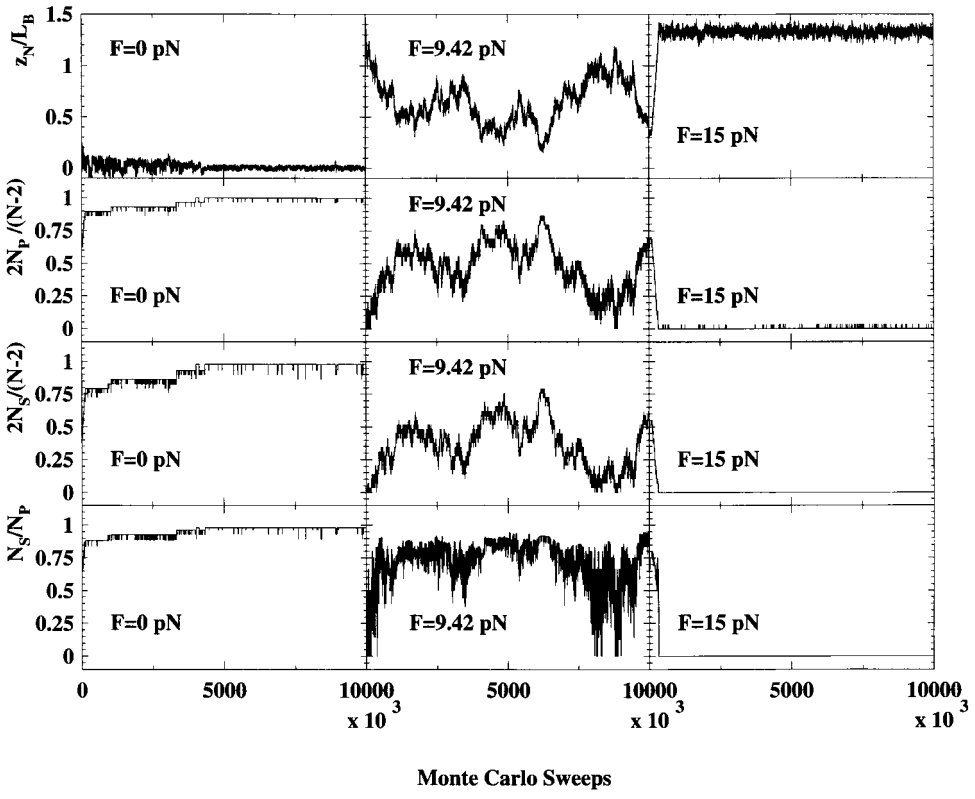

FIGURE 6 Monte Carlo time series of scaled extension z_N/L_B, scaled pairing numbers $2N_P/(N-2)$, scaled stacking pairs $2N_S/(N-2)$, and the ratio of pairs and stacking numbers N_S/N_P for poly(dA-dT) sequence in 150 mM NaCl solution. All the order parameters fluctuate around their thermal equilibrium values when force is far away from critical force $F_c = 9.42$ pN; however, the fluctuations diverge around the critical point.

system. Some techniques, such as the cluster-flipping algorithm (Swendsen and Wang, 1987; Wolff, 1989), have been proposed to alleviate the problem of critical slowing down for a number of spin systems. However, an efficient algorithm for a biopolymer system is still lacking. Keeping in mind the pronounced double-peak structure of the sample action density near the critical point, which is the main reason for the critical slowing down in our simulation, it is possible to construct a new weight factor and enhance the tunneling between these two metastable states at the critical point. The detail into this problem is discussed elsewhere (Y. Zhang and H. Zhou, in preparation).

Sensitivity to pairing rule

In the above calculations, the bases of ssDNA are assumed to be paired according to the so-called standard pairing rule; i.e., the coexisting base pairs are restricted to be either nested or independent (see condition 3 above). It is of interest to see whether and how the mechanical property of the ssDNA chain changes if the bases are allowed to be paired randomly (i.e., neglecting restriction 3 but keeping conditions 1, 2 and 4 above unchanged).

In Fig. 7 *a* we show the comparison of the typical conformations of random sequence at external force $F = 0$ pN, with different pairing rules. Within the random pairing rule, the ssDNA tends to form a locally intersecting base-pairing pattern; within the standard pairing rule, because of the limitation of phase space the conditions of nest and independence lead to the formation of base pairs from spatially distant bases along the strand, which makes the two ends of the chain quite close to each other. So to pull slightly apart the two termini of ssDNA with the standard pairing rule, an additional force is needed to overcome the base-pairing potential at low force. However, this additional force is not necessary for ssDNA with the random pairing rule, because its two ends are usually spatially separated even at $F = 0$ pN (see right column of Fig. 7 *a*).

The processes of stretching the designed sequence can be also different within standard and random pairing rules. In Fig. 7 *b* is the comparison of the poly(dA-dT) chain at external force $F = 9$ pN with different pairing rules. Unlike the independent and nested base-pair pattern with the standard rule (the left column of Fig. 7 *b*), the locally intersecting base pairs can be formed by the random pair rule (see the right column of Fig. 7 *b*). This multiple base-pairing mode makes a larger external force necessary to entirely draw open the secondary structure of ssDNA, and therefore the process of pulling the design ssDNA chain with the random pairing rule should be less incorporative.

As a confirmation, we present the force/extension result of ssDNA within the random pairing rule in Fig. 8. In Fig. 8 *a* is the result of the random sequence in 5 mM $MgCl_2$ solution. Compared with the corresponding result of the standard pairing rule in Fig. 3 *b*, the distance of the two ends of the molecule with the random pairing rule is larger at low external force

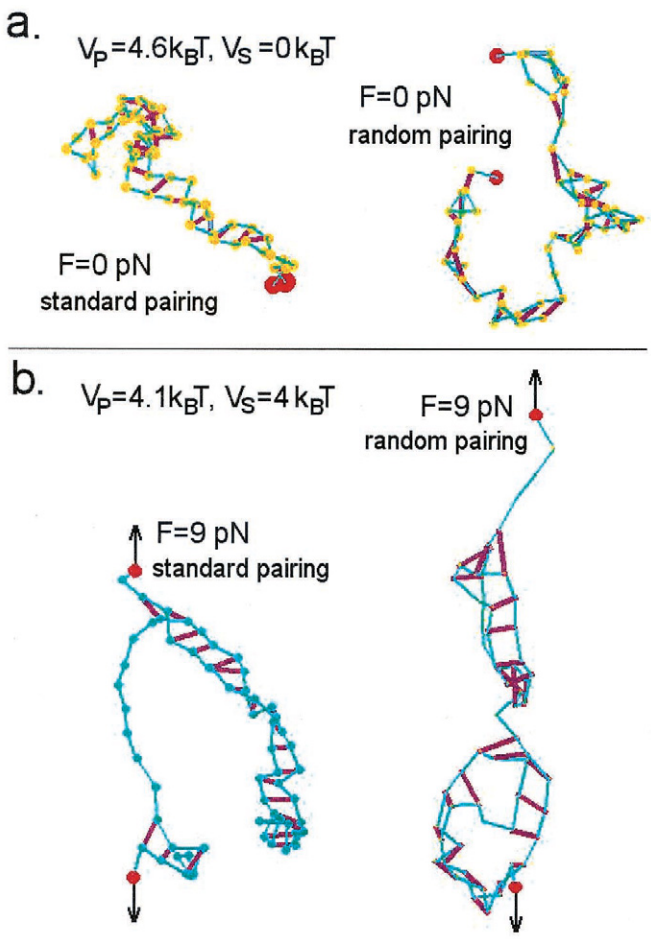

FIGURE 7 Comparison of typical conformations of ssDNA chain with standard and random pairing rules, with model parameters as shown. (*a*) For random DNA sequence in 5 mM $MgCl_2$ solution; (*b*) For poly(dA-dT) DNA sequence in 150 mM NaCl solution. The bases and backbone and hydrogen bonds are expressed in the similar way as that in Fig. 4.

($F < 5$ pN); however, it is smaller at an intermediate force (5 pN $< F <$ 11pN) because of the formation of the local multiple base pairings; the force/extension curves of the two types of pairing rules coincide with each other at high force ($F > 11$ pN) because the chain is relatively straight in this region and little basepair can be formed. In Fig. 8 *b* is the result of poly(dA-dT) ssDNA in 150 mM NaCl solution. As expected, a larger external force was needed to entirely pull open the molecule, and the pulling process is much less incorporative, with the comparison of the standard pairing rule shown in Fig. 3 *c*.

It is obvious that the modeling calculation of the standard pairing rule can fit better to the experimental data of the force/extension characteristics of ssDNA (comparing Figs. 3 and 8). An important difference between these two pairing rules is that the standard rule allows only the planar hairpin structure and therefore avoids the formation of a tertiary pseudo-knot that is allowed by the random rule. This feature is also shared in the three-dimensional arrangement of the RNA molecule. To date, the largest RNA molecule that has been crystallized and whose structure has been determined is the 160-nucleotide P4-P6 domain of the group I ribozyme (Cate et al., 1995). This structure and all other RNA structures that have been solved thus far (see Gutell, 1994) have one thing in common: they are all free of topological knots (VanLoock et al., 1998). We believe that this may be a general property of formed secondary structures of single-stranded polynucleotide molecules.

Concluding remarks

We report a detailed study of MC simulation of pulling ssDNA, in which long-range electrostatic repulsive potential, base pairing, and base-pair stacking interaction are taken into account. To determine the amplitude, or effective linear charge density, of Debye-Hükel electrostatic potential, we first performed a numerical solution of a nonlinear Poisson-Boltzmann equation in both mono- and double-valent electrolytes and match the first-order modified Bessel function with the Poisson-Boltzmann potential in the overlap region. It is found that the effective charge density of both ssDNA and dsDNA molecules in all kinds of salt solution can be well fitted by a simple experience formula,

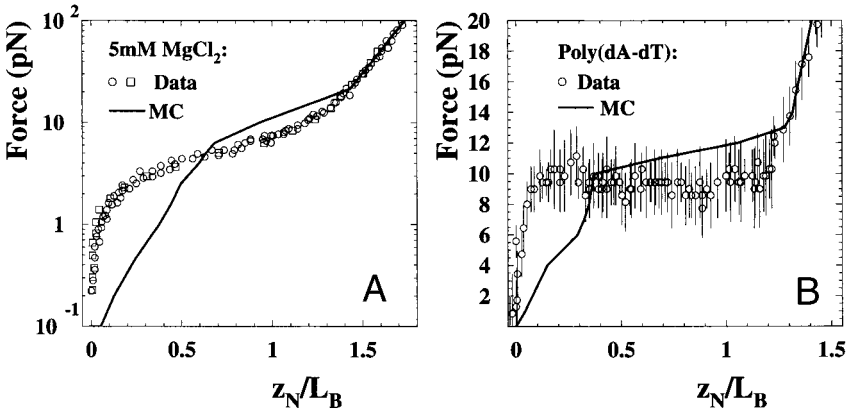

FIGURE 8 External force as the function of distance of two ends of ssDNA. Data are taken from Bustamante et al. (2000), Maier et al. (2000), and Rief et al. (1999). Curves are the modeling results with random pairing rule (see text). The modeling parameters are the same as that shown in Fig. 7. (*a*) For random DNA sequence in 5 mM $MgCl_2$ solution; (*b*) For poly(dA-dT) DNA sequence in 150 mM NaCl solution.

which can be conveniently used in other corresponding studies of electrostatic interactions.

In low-salt solution, the electrostatic repulsive interaction dominates, and there are few formed base pairs because the strong electrostatic repulsive potential excludes the bases from getting close into the Watson-Crick base-pair range. This repulsive interaction makes the chain more easily aligned and more subject to stretching, which is formally equivalent to enlarging the stiffness of the chain. In high-salt solution, the elasticity of the chain is the result of the competition of electrostatic and base-pairing interactions. The pairing interaction can make the secondary structure more difficult to be pulled open than that expected by a pure FJC.

For a designed poly(dA-dT)/poly(dG-dC) chain, the stacking interaction between base pairs encourage base pairs to aggregate into a compact pattern, and a threshold force is necessary to pull back the bulk hairpin structure, characterized by a plateau in the force/extension curve. The height of the plateau is determined by the pairing potential V_P and stacking potential V_S in our model. The best fit to the experimental data shows that $V_P = 4.1k_BT$ and $V_S = 4k_BT$ for the poly(dA-dT) sequence, $V_P = 10.4k_BT$ and $V_S = 6k_BT$ for the poly(dG-dC) sequence. Bearing in mind that each Kuhn length ($\sim$1.6nm) contains about three nucleotide bases, we can infer that the pairing energy of each A-T base pair is $\sim 1.37k_BT$ and that for each G-C base-pair is $\sim 3.47k_BT$. These values are comparable with the measurements of Bockelmann et al. (1997) when they pulled apart the two strands of a dsDNA helix.

In contrast to the gradual elongating of ssDNA of random sequence, the hairpin-coil transition of designed ssDNA is discontinuous. The calculated thermodynamics of stretching a designed ssDNA sequence shows typical critical characteristics. All the order parameters, such as the distance of the two ends of the ssDNA chain, number of pairings, and electrostatic potential, discontinuously jump when the external force passes through the critical force. At the critical point, the fluctuation of the order parameters and the autocorrelation time diverge. This effect, known as critical slowing down, renders the canonical Metropolis MC calculations unreliable. All these features make the designed ssDNA an excellent laboratory for the study of first-order phase transition in a one-dimensional system.

The sensitivity of elongation of ssDNA to the base-pairing rule was also investigated. The release of the restriction of nest (or independence) in the standard pairing rule leads to formation of a tertiary pseudo-knot structure in ssDNA. This locally intersecting base-pairing pattern makes the stretching process of designed DNA sequence less incorporative than that observed in the experimental measurement of Rief et al. (1999). The theoretical calculation of random ssDNA sequence with the random pairing rule also disagrees with the experimental data at low and intermediate external force. These calculations, coinciding with the findings in the three-dimensional arrangement of RNA molecules in the cell, indicate that the nested (or independent) pairing restriction may be a general essential condition for all single-stranded polynucleotide molecules in the process of formation of their secondary structures.

APPENDIX: NUMERICAL SOLUTION OF POISSON-BOLTZMANN EQUATION

Here we outline the general power series technique of solving numerically Poisson-Boltzmann Eq. 1 (Pierce, 1958; Rice and Nagasawa, 1961) for a uniformly charged cylinder immersed in solutions.

By expanding the exponential term on the right-hand side of Eq. 1, the Poisson-Boltzmann equation can written as

$$\nabla^2_{\mathbf{R}}\phi(\mathbf{R}) = \sum_{l=1}^{\infty} A_l \phi(\mathbf{R})^l, \tag{11}$$

where $\phi(\mathbf{R}) = e\psi(\mathbf{r})/k_BT$, $\mathbf{R} = \kappa\mathbf{r}$, $\kappa = 4\pi/Dk_BT)\ \Sigma_{i=1}^{n}\ c_i(v_ie)^2$, and $A_l = \Sigma_{i=1}^{n}\ (-1)^{l+1}c_iv_i^{l+1}/\Sigma_{i=1}^{n}\ l!c_iv_i^2$. In case the electrostatic potential is rather small relative to k_BT, terms higher than the square in the expansion may be neglected, and Eq. 11 assumes the Debye-Hükel form:

$$\nabla^2_{\mathbf{R}}\phi(\mathbf{R}) = \phi(\mathbf{R}), \tag{12}$$

which can be solved explicitly.

Let's assume that $\phi(\mathbf{R})$ of Eq. 11 can be expressed in a series of

$$\phi(\mathbf{R}) = \sum_{m=1}^{\infty} C^m \phi_m(\mathbf{R}), \tag{13}$$

where C is a constant to be determined from the boundary condition of the ssDNA molecule. For 1:1 electrolytes such as NaCl, because the terms containing even powers of $\phi(\mathbf{R})$ in Eq. 11 cancel out, only odd terms need to be preserved in Eq. 13. However, for solutions containing asymmetrical electrolytes such as $MgCl_2$, all of the sequential terms of expansion must be retained up to the required order.

Substituting Eq. 13 into Eq. 11, we have

$$\nabla^2_{\mathbf{R}}\phi_m(\mathbf{R}) = \phi_m(\mathbf{R}) + g_m(\mathbf{R}), \tag{14}$$

where $g_m(\mathbf{R})$ is a function of lower order $\phi_i(\mathbf{R})$ ($i = 1, \ldots, m-1$). Because $g_1(\mathbf{R}) = 0$, the initial equation of $\Phi_1(\mathbf{R})$ corresponds the Debye-Hükel Eq. 12. Its solution in the cylinder coordinate system is the zero-order modified Bessel function $K_0(R)$ of the second kind (see also Eq. 3), where $R = \kappa r$ and both R and r are radial distance from the axis of the cylinder. Higher-order $\Phi_m(R)$ in the cylinder coordinate system can be calculated iteratively (Sugai and Nitta, 1973):

$$\phi_M(R) = I_0(R)\int_{\infty}^{R} tK_0(t)g_m(t)dt - K_0(R)\int_{\infty}^{R} tI_0(t)g_m(t)dt, \tag{15}$$

where $I_0(R)$ is the first kind modified Bessel function.

To determine the constant C in Eq. 13, we notice that the electrical equilibrium between the DNA cylinder and electrolyte should be reached under the strong electrostatic forces. According to the Poisson-Boltzmann equation, the excess charge density of electrolyte is $\rho(r) = \Sigma_{i=1}^{n}\ v_iec_i \exp(-v_i\psi(r))$. For the ssDNA cylinder, there is one phosphate group along each base length of $\sim h = 0.6$ nm. So we have (Delrow et al., 1997)

$$\int_{\tau_0}^{\infty} 2\pi rh\rho(r)dr + Q = 0, \tag{16}$$

where we have taken $Q = -e$ and $r_0 = 0.5$nm (Saenger, 1984). For the dsDNA cylinder, the corresponding parameters are $h = 0.34$ nm, $Q = -2e$, and $r_0 = 1.2$ nm.

H.Z. acknowledges financial support from the Alexander von Humboldt Foundation.

REFERENCES

Bockelmann, U., B. Essevaz-Roulet, and F. Heslot. 1997. Molecular stick-slip motion revealed by opening DNA with piconewton force. *Phys. Rev. Lett.* 79:4489–4492.

Brenner, S. L., and V. A. Parsegian. 1974. A physical method for deriving the electrostatic interaction between rod-like polyions at all mutual angles. *Biophys. J.* 14:327–334.

Bundschuh, R., and T. Hwa. 1999. RNA secondary structure formation: a solvable model of heteropolymer folding. *Phys. Rev. Lett.* 83:1479–1482.

Bustamante, C., J. F. Marko, E. D. Siggia, and S. B. Smith. 1994. Entropic elasticity of lambda-phage DNA. *Science.* 265:1599–1601.

Bustamante, C., S. B. Smith, J. Liphardt, and D. Smith. 2000. Single-molecule studies of DNA mechanics. *Curr. Opin. Struct. Biol.* 10:279–285.

Cate, J. H., A. R. Gooding, E. Podell, K. Zhou, B. L. Golden, C. E. Kundrot, T. R. Cech, and J. A. Doudna. 1995. Crystal structure of a group I ribozyme domain: principles of RNA packing. *Science.* 273:1678–1685.

Clausen-Schaumann, H., M. Seitz, R. Krautbauer, and H. E. Gaub. 2000. Force spectroscopy with single bio-molecules. *Curr. Opin. Chem. Biol.* 4:524–530.

Cluzel, P., A. Lebrun, C. Heller, R. Lavery, J. -L. Viovy, D. Chatenay, and F. Caron. 1996. DNA: an extensible molecule. *Science.* 271:792–794.

Delrow, J. J., J. A. Gebe, and J. M. Schurr. 1997. Comparison of hard-cylinder and screen coulomb interactions in the modeling of supercoiled DNAs. *Biopolymers.* 42:455–470.

Gradshteyn, I. S., and I. M. Ryzhik. 1980. Table of Integral, Series, and Products. Academic Press, New York.

Gutell, R. R. 1994. Collection of small subunit (16S- and 16S-like) ribosomal RNA structures. *Nucleic Acids Res.* 22:3502–3507.

Hansmann, U. H. E., and Y. Okamoto. 1997. Generalized-ensemble Monte Carlo method for systems with rough energy landscape. *Phys. Rev. E.* 56:2228–2233.

Higgs, P. G. 1996. Overlaps between RNA secondary structures. *Phys. Rev. Lett.* 76:704–707.

Lu, H., B. Isralewitz, A. Krammer, V. Vogel, and K. Schulten. 1998. Unfolding of titin immunoglobulin domains by steered molecular dynamics simulation. *Biophys. J.* 75:662–671.

Maier, B., D. Bensimon, and V. Croquette. 2000. Replication by a single DNA polymerase of a stretched single-stranded DNA. *Proc. Natl. Acid. Sci. U.S.A.* 97:12002–12007.

Marko, J. F., and E. D. Siggia. 1995. Stretching DNA. *Macromolecules.* 28:8759–8770.

Metropolis, N., A. W. Rosenbluth, M. N. Rosenbluth, and A. H. Teller. 1953. Equation of state calculations by fast computing machines. *J. Chem. Phys.* 21:1087–1092.

Montanari, A., and M. Mezard. 2000. Pulling hairpinned polymers. *Phys. Rev. Lett.* 86:2178–2181.

Pierce, P. 1958. Ph.D. thesis. Yale University, New Haven, CT.

Rice, S. A., and M. Nagasawa. 1961. Polyelectrolyte Solutions. Academic Press, New York.

Rief, M., H. Clausen-Schaumann, and H. E. Gaub. 1999. Sequence-dependent mechanics of single DNA molecules. *Nat. Struct. Biol.* 6:346–349.

Rief, M., M. Gautel, F. Oesterhelt, J. M. Fernandez, and H. E. Gaub. 1997. Reversible unfolding of individual titin immunoglobulin domains by AFM. *Science.* 276:1109–1112.

Saenger, W. 1984. Principles of Nucleic Acid Structure. Springer-Verlag, New York.

Smith, S. B., Y. Cui, and C. Bustamante. 1996. Overstretching B-DNA: the elastic response of individual double-stranded and single-stranded DNA molecules. *Science.* 271:795–799.

Smith., S. B., L. Finzi, and C. Bustamante. 1992. Direct mechanical measurements of elasticity of single DNA molecules by using magnetic beads. *Science.* 258:1122–1126.

Schellman, J. A., and D. Stigter. 1977. Electrical double layer, zeta potential, and electrophoretic charge of double-stranded DNA. *Biopolymers.* 16: 1415–1434.

Stigter, D. 1977. Interactions of highly charged colloidal cylinders with applications to double-stranded DNA. *Biopolymers.* 16:1435–1448.

Stigter, D., and K. A. Dill. 1993. Theory for second virial coefficients of short DNA. *J. Phys. Chem.* 97:12995–12997.

Strick, T. R., J. F. Allemand, D. Bensimon, and V. Croquette. 1996. The elasticity of a single supercoiled DNA molecule. *Science.* 271:1835–1837.

Sugai, S., and K. Nitta. 1973. Surface electric potential on rod-like polyelectrolyte. *Biopolymers.* 12:1363–1376.

Swendsen, R. H., and J. S. Wang. 1987. Nonuniversal critical dynamics in Monte Carlo simulations. *Phys. Rev. Lett.* 58:86–88.

VanLoock, M. S., B. A. Harris, and S. C. Harvey. 1998. To knot or not to knot? Examination of 16S ribosomal RNA models. *J. Biomol. Struct. Dyn.* 16:709–713.

Vologodskii, A. V. 1994. DNA extension under the action of an external force. *Macromolecules.* 27:5623–5625.

Vologodskii, A. V., S. D. Levene, K. V. Klenin, M. Frank-Kamenetskii, and N. R. Cozzarelli. 1992. Conformational and thermodynamic properties of supercoiled DNA. *J. Mol. Biol.* 227:1224–1243.

Wilde, R. E., and S. Singh. 1998. Statistical Mechanics: fundamental and Modern Applications. John Wiley and Sons, New York.

Wolff, U. 1989. Collective Monte Carlo updating for spin systems. *Phys. Rev. Lett.* 62.:361–364.

Wuite G. J., S. B. Smith, M. Young, D. Keller, and C. Bustamante. 2000. Single molecule studies of the effect of template tension on T7 DNA polymerase activity. *Nature.* 404:103–106.

Zhang, Y. 2000. New approach to Monte Carlo calculation of buckling of supercoiled DNA loops. *Phys. Rev. E.* 62:R5923–R5926.

Zhang, Y., H. J. Zhou, and Z. C. Ou-Yang. 2000. Monte Carlo implementation of supercoiled double-stranded DNA. *Biophys. J.* 78:1979–1987.

Zhou, H. J., and Y. Zhang. 2001. Pulling hairpinned polynucleotide chains: does base-pair stacking interaction matter? *J. Chem. Phys.* 114:8694–8700.

Zhou, H. J., Y. Zhang, and Z. C. Ou-Yang. 1999. Bending and basestacking interactions in double-stranded DNA. *Phys. Rev. Lett.* 82:4560–4563.

Zhou, H. J., Y. Zhang, and Z. C. Ou-Yang. 2000. Elastic property of single double-stranded DNA molecules: theoretical study and comparison with experiments. *Phys. Rev. E.* 62:1045–1058.

Zhou, H. J., Y. Zhang, and Z. C. Ou-Yang. 2001. Stretch-induced hairpin-coil transitions in designed polynucleotide chains. *Phys. Rev. Lett.* 86:356–359.